Journal Computational Simulation 9[20]1-17: e2092017
Article

Dynamic control analysis by simulation of the main components of a Hall Effect thruster

Análisis dinámico del control mediante simulación de los componentes principales un propulsor de efecto Hall

Aburto–Policarpo Gethsi[a], Castillo-Sánchez Martín*[b] and López-Cárdenas Rodrigo[c]

[a] Instituto Politécnico Nacional • 0009-0001-2050-720X
[b] Instituto Politécnico Nacional • 0000-0002-2563-3395 • 36671
[c] Instituto Politécnico Nacional • 0009-0007-2628-9147 • 162756

SECIHTI classification:

Area: Engineering
Field: Technological sciences
Discipline: Space technology
Subdiscipline: Spaceships

https://doi.org/10.35429/JCS.2025.9.20.2.1.17
Article History:
Received: June 30, 2025
Accepted: December 15, 2025

* ✉ [mcastillos@ipn.mx]

Abstract

The aim of this research work is to analyze, through the simulation of the controllers using Simulink ™, the behavior of the main components that make up a Hall effect electric thruster used in a spacecraft, these are: Magnetic field, Voltage and Injector, the simulated controls for the components were P, I, PI, PD, PID controls, it was found that the PI and PID controllers are the most suitable to regulate the magnetic field, due to the precise tracking of the reference, unlike the PD controller, whose abrupt changes make it physically unfeasible. Regarding voltage control, the PI controller stands out for its balance between efficiency and physical feasibility, while the PD and PID controllers, although acceptable, present excessively rapid variations that hinder their real implementation. Likewise, in scenarios where a faster adjustment is prioritized, the PID could be considered, as long as its practical limitations are evaluated.

Objectives	Methodology	Contribution
Controller simulation Hall effect electric thruster: Magnetic field Voltage Injector 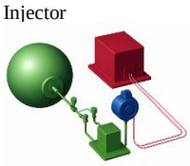 **Magnetic field** **Fuel** **Propellant**	Magnetic Field $H(s) = \frac{200}{s+1}$ Voltage $H(s) = \frac{2000}{s^2+s+1}$ Injector $H(s) = \frac{k}{s+1}$	PI and PID controllers are best suited for regulating magnetic fields, injector, and voltage control.

Controllers, Hall effect, spacecraft

Resumen

El objetivo de este trabajo de investigación es analizar mediante la simulación de los controladores mediante Simulink™, el comportamiento de los componentes principales que conforman un propulsor eléctrico de efecto Hall utilizado en una nave espacial, estos son: Campo magnético, Tensión e Inyector, los controles simulados para los componentes fueron controles P, I, PI, PD, PID, se encontró que los controladores PI y PID son los más adecuados para regular el campo magnético, debido a el seguimiento preciso de la referencia, a diferencia del controlador PD, cuyos cambios abruptos lo hacen físicamente inviable. En cuanto al control de tensión, el controlador PI destaca por su balance entre eficiencia y factibilidad física, mientras que los controladores PD y PID, aunque aceptables, presentan variaciones demasiado rápidas que dificultan su implementación real. Así mismo en escenarios donde se priorice un ajuste más rápido, el PID podría considerarse, siempre y cuando se evalúen sus limitaciones prácticas.

Objetivos	Metodología	Contribución
Simulación de controladores propulsor eléctrico de efecto Hall: Campo magnético Voltaje Inyector 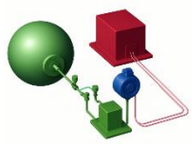 **Alimentación** **Propelente** **Propulsor**	Campo Magnético $H(s) = \frac{200}{s+1}$ Tensión $H(s) = \frac{2000}{s^2+s+1}$ Inyector $H(s) = \frac{k}{s+1}$	Los controladores PI y PID son los más adecuados para regular campos magnéticos, el inyector, y el control de voltaje.

Controladores, efecto Hall, nave espacial

Area: Promotion of frontier research and basic science in all fields of knowledge

Citation: Aburto–Policarpo Gethsi, Castillo-Sánchez Martín and López-Cárdenas Rodrigo [2025]. Dynamic control analysis by simulation of the main components of a Hall Effect thruster. Journal Computational Simulation. 9[20] 1-17: e20920117

Introduction

Electric propulsion is a technology designed to achieve thrust with high exhaust velocities, resulting in a reduction in the amount of propellant required for a given space mission or application compared to chemical propulsion. The reduced propellant mass can significantly decrease the launch mass of a spacecraft or satellite, leading to lower costs by using smaller launch vehicles to deliver a desired mass into a specific orbit or to a target in deep space. In general, electric propulsion (EP) encompasses any propulsion technology in which electricity is used to increase the propellant's exhaust velocity. There are many figures of merit for electric propellants, but mission and application planners are primarily interested in thrust, specific impulse, and overall efficiency when relating propellant performance to mass delivered and the change in spacecraft velocity during thrust periods. (Goebel, D. M. 2008. Merino, M. 2016. Hey, F. G. 2018).

There are various types of electric thrusters used by space agencies and research centers, each with specific characteristics in terms of thrust, specific impulse, and efficiency. However, there is a need to optimize these parameters based on the spacecraft's mass and the change in velocity during thrust periods. The main problem lies in the need for detailed characterization and simulation of this type of electric thruster in terms of its efficiency, power requirements, voltage, current intensity, and specific impulse.

This work analyzes, through the simulation of the controllers of a Hall effect thruster using mathematical software, the design and specific characteristics of an electric propulsion system in a spacecraft, considering thrust, power and specific impulse in different types of space missions (ESA. 2002. Lev, D. 2019).

Hall Effect Drivers (HET)

When a current flows in a conductor or semiconductor and a magnetic field is applied perpendicular to the current, a voltage is generated across the material in a direction perpendicular to the planes containing the current and the magnetic field, as shown in Figure 1. This voltage is known as the Hall voltage, and the phenomenon is known as the Hall effect. (Jiles, D. 2001).

Box 1

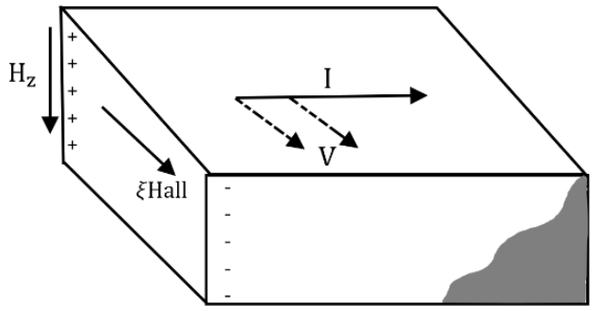

Figure 1

Hall electromagnetic field. H is the magnetic field, I, is the conventional current, ξHall is the Hall field, and v is the electron velocity. Adapted from (Jiles, D. 2001)

The Hall effect thruster is an electrostatic ion accelerator that uses a cross-field cycloidal ion discharge accelerated by an electrostatic field in the thrust stream to generate plasma. The plasma electrons interact with a magnetic field to produce the electrostatic field described by the Hall effect. Perpendicular fields electrostatically accelerate the ions to high speeds.

The magnetic coils are positioned perpendicular to the main discharge for simplicity, and some additional control can be implemented. This type of thruster is both an electrostatic and electromagnetic EP system. The electrons follow a particular closed drift path perpendicular to the current flow and the magnetic field (Hall effect). The structure of a Hall thruster consists of an annular discharge chamber with a radial magnetic field between a cylindrical ferromagnetic pole and an external ferromagnetic ring (Figure 2).

The chamber forms an outlet for the accelerated ions at one end. Electrons travel from the cathode to the anode in an externally applied electric field. The radial magnetic field generates a perpendicular force from both fields, causing them to drift in an azimuthal direction (hence the Hall current). When the electron moves toward the anode (accelerated), its spin radius increases compared to when it moves toward the cathode (decelerated), resulting in a net azimuthal drift (Hall effect). The electrons are efficiently trapped in an azimuthal orbit near the area of maximum field strength. The axial mobility of the electrons is eradicated, allowing the plasma to maintain a very high electric field along the axis of the discharge chamber.

ISSN: 2523-6865
RENIECYT-SECIHTI: 1702902

Aburto–Policarpo Gethsi, Castillo-Sánchez Martín and López-Cárdenas Rodrigo [2025]. Dynamic control analysis by simulation of the main components of a Hall Effect thruster. Journal Computational Simulation. 9[20] 1-17: e20920117
https://doi.org/10.35429/JCS.2025.9.20.2.1.17

There is an external cathode, which provides additional electrons to neutralize the accelerated ions in the discharge chamber. (Poonam T. 2020).

Hall thrusters require relatively simple power conditioning and provide a desirable specific impulse range, but xenon is the only propellant that can be used safely. These thrusters optimize performance at very low power. Exhaust velocities can reach over 65,000 m/s, and their power range extends from around 200 W to tens of kW. They have propellant efficiencies of over 50%, thrust efficiencies of around 45–55%, and thrust exceeding 70 mN. They also have a high specific impulse of 1,000–8,000 s. There is a 5% loss in specific impulse due to propellant flow in the hollow cathode.

Starting point parameters and scaling laws

The rocket equation reduces to a propellant weight problem: as propellant is added to a spacecraft, the mass of the system increases, and increasingly longer propellant burns are required to accelerate the increased mass of the system.

This establishes a practical upper limit on the amount of fuel carried, since at a certain point only marginal changes in velocity (Δv) can be achieved by adding more propellant. The momentum transfer efficiency of a propellant can be maximized by maximizing the propellant's exit velocity, vex; this, in turn, reduces the amount of propellant required to achieve a desired Δv. (Oh B. 2023).

Box 2

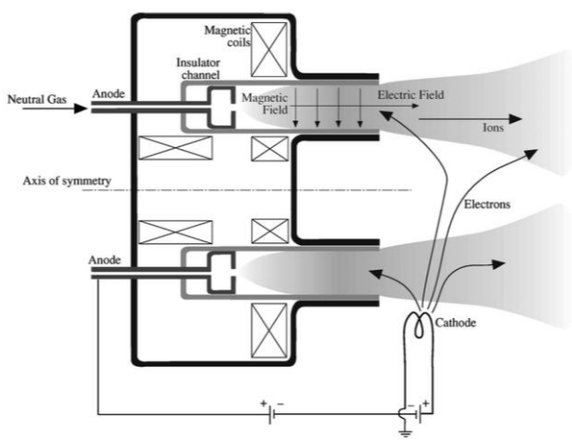

Figure 2
Physical diagram of a Hall effect thruster. (Adapted from Poonam T. 2020)

Two thrusters operating at a similar voltage will accelerate ions through a similar potential, resulting in similar escape velocities (neglecting specific design losses) and therefore similar specific impulse. These scaling laws are:

$$P \propto R^2 \quad [1]$$
$$T \propto R^2 \quad [2]$$
$$W \propto R \quad [3]$$

Where R represents the outer radius of the propeller channel and W represents the channel width (the difference between the outer and inner radii).

Concepts of Electric and Magnetic Fields

The propellant is ionized by bombarding it with electrons trapped in the main channel.

The electrons are trapped by a radial magnetic field. An axial electric field is then applied, causing the electrons to drift.$\vec{E} \times \vec{B}$, This results in an azimuthal velocity (a drift-enabled Hall current). The purpose of the device's electric field is to transport electrons from the cathode to the channel and accelerate the ionized propellant away from the propellant. (Oh B. 2023). In electric propulsion, especially in Hall-type thrusters and some magneto plasmic thrusters, the drift phenomenon $\vec{E} \times \vec{B}$ It is a determining factor in generating thrust.

In a Hall thruster, it is established that:

– An electric field $\vec{E}$ radial between the anode (interior) and the cathode (exterior).

– A magnetic field$\vec{B}$ axial (perpendicular to the electric field).

The combination of these two fields generates a drift velocity.

The principles of drift$\vec{E} \times \vec{B}$ They can be conceptualized as follows: Consider a region of space with a uniform magnetic field. A charge moving in this field will travel in endless circles. Now, consider the same configuration with a uniform electric field oriented perpendicular to the magnetic field. When the charge is at a point of higher electric potential, it will possess less kinetic energy and travel more slowly; conversely, at a point of lower electric potential, it will travel more quickly.

ISSN: 2523-6865
RENIECYT-SECIHTI: 1702902

Aburto–Policarpo Gethsi, Castillo-Sánchez Martín and López-Cárdenas Rodrigo [2025]. Dynamic control analysis by simulation of the main components of a Hall Effect thruster. Journal Computational Simulation. 9[20] 1-17: e20920117
https://doi.org/10.35429/JCS.2025.9.20.2.1.17

This causes the particle to alternate between a narrow orbit and a large orbit (in regions of lower and higher potential, respectively) and results in a drift perpendicular to both the electric and magnetic fields. Figure 3 shows a sample trajectory of a particle trapped within such a field. This phenomenon is known as drift $\vec{E} \times \vec{B}$ and it is the central mechanism that allows electrons to be trapped inside the thruster channel in an azimuthal flow (this is the Hall current that gives Hall thrusters their characteristic name) (Oh B. 2023).

Box 3

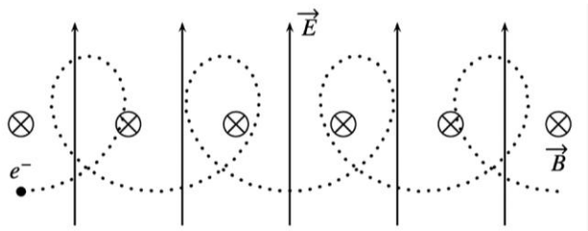

Figure 3

Cycloidal trajectory of an electron undergoing drift $\vec{E} \times \vec{B}$ in a uniform electric and magnetic field. (Taken from Oh B. 2023)

A useful way to characterize the magnetic field in a propellant is by the radii of gyration of the ions present in the system (this radius is known in the field as the Larmor radius). The Larmor radius for a generic charge in a magnetic field can be found as:

$$r_q = \frac{mv_\perp}{qB} \quad [4]$$

Where r_q is the Larmor radius for a particle of mass m and charge q, with velocity perpendicular to the field B of magnitude v⊥. The Larmor radius can be calculated by knowing the magnetic field strength along with the particle's velocity, mass, and charge. For particles in a Hall thruster, the Larmor radii are:

$$r_e = \frac{1}{B}\sqrt{\frac{8m_e kT_e}{\pi e}} \quad [5]$$

$$r_i = \frac{1}{B}\sqrt{\frac{2m_i V_b}{e}} \quad [6]$$

Where r_e and r_i are the Larmor radii of an electron and an ion, respectively; B is the radial magnetic field strength; me and mi are the masses of an electron and an ion, respectively; T_e is the temperature of the electron in units of eV; k is Boltzmann's constant; V_b is the propellant beam voltage; and e, is the fundamental load (Oh B. 2023).

Propellant Selection and Channel Length

Neutral propellant is dispensed from a diffuser at the bottom of the channel. As the neutrals diffuse through the channel, they come into contact with the cloud of high-energy electrons trapped in the ionization region. Maximizing the amount of ionized propellant maximizes propellant efficiency, dictating a channel length that must be significantly longer than the mean ionizing free path, but not so long as to cause performance losses due to interactions with a larger surface area. Generally, this length is chosen to be of the same order of magnitude as the mean free path length. One calculation method is:

$$\lambda = \frac{v_n}{n_e(\sigma_i v_e)} \quad [7]$$

Where v_n is the axial velocity of a neutral propellant atom, n_e is the electron density of the channel and $\langle \sigma_i v_e \rangle$ represents the ionization "cross-section" (which quantifies the probability of ionization) of the neutral propellant for collisions with electrons at a particular electron temperature. The amount v_n It can be calculated using Bernoulli's equation, given the parameters of a particular feed piping system and the propellant flow properties. The ionization cross-section, $\langle \sigma_i v_e \rangle$, It is an experimentally derived value that varies with the type of propellant and the energy level of the electrons. (Oh B. 2023).

Methodology

Modeling the Hall Effect Thruster

In the electric propulsion model, each main system component is represented by a transfer function in the Laplace domain. The constant appearing in the numerator of each function has a specific physical meaning depending on the block it corresponds to. (Sánchez, J. 2015).

ISSN: 2523-6865
RENIECYT-SECIHTI: 1702902

Aburto–Policarpo Gethsi, Castillo-Sánchez Martín and López-Cárdenas Rodrigo [2025]. Dynamic control analysis by simulation of the main components of a Hall Effect thruster. Journal Computational Simulation. 9[20] 1-17: e20920117
https://doi.org/10.35429/JCS.2025.9.20.2.1.17

Injector

Based on the propeller dynamics, a simplified differential equation is formulated to model the opening and closing of a propeller, considering only the valve size. The injector's transfer function is described as:

$$H(s) = \frac{k}{s+1} \quad [8]$$

In this context, *k* this represents the mass flow gain injected per unit of input signal. Physically, this means that, for a given control stimulus (electrical potential or current), the injector is able to transfer a proportional amount of mass to the propulsion system.

A higher value of *k* It increases the mass flow rate in response to the same input. A lower value reduces the injection capacity.

In a linear system described by the differential equation:

$$y'(t) + y(t) = kx(t) \quad [9]$$

and its corresponding transfer function in the frequency domain described above:

$$H(s) = \frac{k}{s+1} \quad [10]$$

The parameter k, this represents the system gain, a proportionality factor that directly affects the amplitude of the system's response to a given input.

When the input is a unit step, that is, $x(t) = u(t)$, The output in the time domain is expressed as:

$$y(t) = k(1 - e^{-t})u(t) \quad [11]$$

The response to the unit step input is an increasing exponential function that asymptotically approaches the value of *k*.

Magnetic Field

The magnetic field transfer function is expressed as:

$$H(s) = \frac{200}{s+1} \quad [12]$$

In this case, the constant value of 200 in the numerator reflects the strength of the magnetic field generated per unit of input signal (current applied to the electromagnet, for example). Physically, an increase in this value would indicate a stronger magnetic field, which would increase control over the flow of charged particles in the propellant. A higher value of *k* This would imply a higher field density for the same current.

A lower value would reduce the magnetic control over the particles.

The time output for equation (2.16) is:

$$y(t) = 200(1 - e^{-t})u(t) \quad [13]$$

Therefore, the effects of this change in the numerator of the transfer function are:

- The final amplitude of the system changes from *k* to 200.
- The system continues to reach 63% of its final value in approximately one second (time constant), since this constant depends on the denominator (s+1).
- It is an exponentially increasing response that asymptotically reaches 200.

Voltage

However, we now have a second-order transfer function that expresses the voltage given by:

$$H(s) = \frac{2000}{s^2 + s + 1} \quad [14]$$

The presence of s2 in the denominator significantly modifies the system's behavior compared to the previous case.

If we compare it to the standard model of a second-order system:

$$H(s) = \frac{K}{s^2 + 2\zeta\omega_n s + \omega_n^2} \quad [15]$$

Here, the constant of 2000 in the numerator represents the gain in particle acceleration when a control signal is applied.

ISSN: 2523-6865
RENIECYT-SECIHTI: 1702902

Aburto–Policarpo Gethsi, Castillo-Sánchez Martín and López-Cárdenas Rodrigo [2025]. Dynamic control analysis by simulation of the main components of a Hall Effect thruster. Journal Computational Simulation. 9[20] 1-17: e20920117
https://doi.org/10.35429/JCS.2025.9.20.2.1.17

This results in a higher ejection velocity, and therefore, greater thrust from the propellant. Increasing k implies a more powerful acceleration of the particles, increasing the thrust.

Reducing k would decrease acceleration effectiveness.

We can observe that:

- The profit is represented by the numerator, that is, k =2000.
- The denominator contains the terms corresponding to the damping coefficients (ζ) and the natural frequency (ω_n).

The parameter k in each block of the system defines the direct relationship between the input signal and the physical response of the component:

- In the injector: determines the mass flow.
- In the magnetic field: it regulates the field intensity.
- In tension: it controls the acceleration of particles.

Proper adjustment of this parameter allows for optimization of the performance of the electric propulsion system in terms of efficiency and thrust.

PID Control

The objective of any control system is, given a certain system and a certain amount of information available based on a series of measurements of some of its signals, to try to determine certain feasible control inputs so that the system variable to be controlled follows a certain reference signal as exactly as possible, despite the influence of possible disturbances, measurement errors, and variations in the system load. (Moreno, L. 2003).

Figure 4 shows a general process control scheme G_p (the process G_p refers to the transfer function that represents the dynamics of a physical system that is to be controlled), where:

r: is the control reference
u: is the control signal
y: is the output of the control system

Box 4

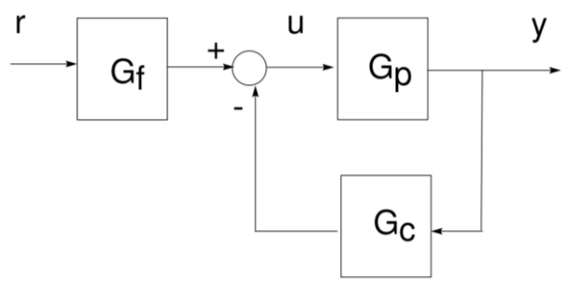

Figure 4
Block diagram of a general control scheme (Adapted from Moreno, L. 2003)

In this scheme, the control signal is:

$$U(s) = G_f(s)R(s) - G_C(s)Y(s) \quad [16]$$

A portion of the control signal formed by a controller can be seen.G_C located in the feedback loop and another by a filter G_f at the system entrance (García H. 2010). To obtain the transfer function, we have:

$$Y(s) = U(s)G_p(s)$$
$$U(s) = G_f(s)R(s)G_p(s) - G_C(s)Y(s)G_p(s)$$
$$Y(s)[1 + G_C(s)G_p(s)] = G_f(s)R(s)G_p(s)$$

The control scheme in Figure 4, has the following expression for the joint transfer function of the entire system: (Moreno, L. 2003)

$$\frac{Y(s)}{R(s)} = G_f(s)\frac{G_p(s)}{1 + G_p(s)G_c(s)} \quad [17]$$

In this expression, it can be observed that the filtering termG_f it directly affects the steady-state gain of the feedback system, as well as its poles and zeros, since it is located in the main chain before the feedback loop. However, it does not alter the positions of the poles and zeros of the feedback loop, except in the case of pole-zero cancellations between G_f and the feedback loop transfer function.

On the other hand, the termG_c, being located in the feedback loop significantly affects the positions of the poles in the closed-loop system, substantially altering the system's dynamics. To simplify somewhat, one can think that while with the design of G_f We seek to improve or adjust the steady-state response of the system, with G_c the aim is to adjust the transient response (Moreno, L. 2003).

ISSN: 2523-6865
RENIECYT-SECIHTI: 1702902

Aburto–Policarpo Gethsi, Castillo-Sánchez Martín and López-Cárdenas Rodrigo [2025]. Dynamic control analysis by simulation of the main components of a Hall Effect thruster. Journal Computational Simulation. 9[20] 1-17: e20920117
https://doi.org/10.35429/JCS.2025.9.20.2.1.17

A particular case of this control structure occurs when $G_f = G_c$. In this case, design freedom is reduced since only one transfer function is available. Therefore, the control scheme is simplified to that shown in diagram (a) of Figure 5, and can also be expressed using the equivalent diagram (b).

Box 5

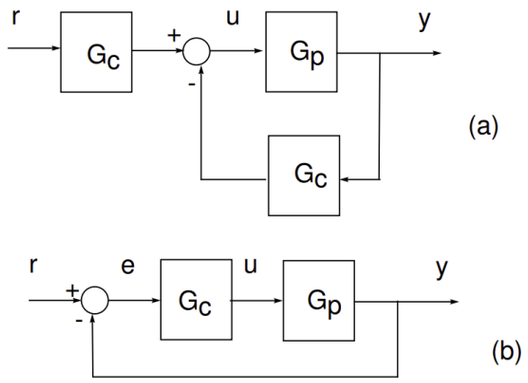

Figure 5
Controller in the main loop (Adapted from Moreno, L. 2003)

This equivalent scheme (b) is what can be called the classic control scheme. PID control is included within this group of controllers. (García H. 2010).

The PID (Proportional-Integral-Derivative) controller is the most widely implemented control algorithm in industry. The vast majority of feedback loops operate under this scheme or one of its adaptations. Its implementation can take various forms, either as a standalone unit or as an integral part of more complex systems, such as Direct Digital Control (DDC) or hierarchical distributed control architectures. (Åström K. 2009).

Despite advances in more complex control strategies, PID control remains fundamental in the basic stage of many industrial processes. In fact, in numerous cases, it is still the most widely used technique due to its effectiveness and versatility. (Moreno, L. 2003).

The PID algorithm

The PID algorithm can be written as:

$$u(t) = K\left[e(t) + \frac{1}{T_i}\int_0^t e(\tau)d\tau + T_d\frac{de(t)}{dt}\right] \quad [18]$$

Where u is the control signal and e is the control error ($e = y_{sp} - y$).

The control signal is thus a sum of three terms: the P-term (which is proportional to the error), the I-term (which is proportional to the integral of the error), and the D-term (which is proportional to the derivative of the error). The controller parameters are the proportional gain. K, the integral time T_i, and derivative time T_d. (Åström K. 2009).

It can be observed that if the integral time constant becomes infinite, the integral action disappears, and if the derivative time constant becomes zero, the derivative action disappears.

The transfer function of the PID controller is as follows: (Moreno, L. 2003).

$$\frac{U(s)}{E(s)} = K\left(1 + \frac{1}{T_i s} + T_d s\right) = \frac{K(1 + sT_i + s^2T_iT_d)}{sT_i} \quad [19]$$

In this controller, the adjustment aims to determine the positions of the two zeros of the transfer function and its static gain, so that the desired design specifications of the system are met as closely as possible (Moreno, L. 2003). A real PID controller will have the following form:

$$G_c(s) = K\frac{1 + sT_i + s^2T_iT_d}{(1 + sT_i)(1 + sT_d)} \quad [20]$$

The regulator parameters can be adjusted in two ways:

1. Empirically

This involves experimentally adjusting the values until the desired response is achieved. This method can be excessively slow in many systems, especially if the response time is long. To avoid this problem, Ziegler-Nichols methods are used. Based on very simple measurements observed in the system's response, these methods provide theoretical values for the controller parameters. These values are taken as a reference, and further fine-tuning is then performed from them. These methods, and others derived from them, are widely used in industry, both for purely manual tuning and in industrial PID controllers with self-tuning systems.

ISSN: 2523-6865
RENIECYT-SECIHTI: 1702902

Aburto–Policarpo Gethsi, Castillo-Sánchez Martín and López-Cárdenas Rodrigo [2025]. Dynamic control analysis by simulation of the main components of a Hall Effect thruster. Journal Computational Simulation. 9[20] 1-17: e20920117
https://doi.org/10.35429/JCS.2025.9.20.2.1.17

2. Theoretically

This involves analytically determining the regulator values. It requires explicit knowledge of the process transfer function (Moreno, L. 2003).

Proportional Action

In the case of pure proportional control, the control law given by Equation 9 reduces to:

$$u(t) = Ke(t) + u_b \quad [21]$$

The control action is simply proportional to the control error. The variableu_b It's a polarization or a reset. When the control error e is zero, the control signal takes the value u(t) = u_b. Polarization u_b often fixes on ($u_{max} + u_{min}$)/2, but it can sometimes be manually adjusted so that the steady-state control error is zero at a given setpoint (Åström K. 2009).

Integral Action

The primary function of integral action is to ensure that the process output matches the setpoint at steady state. With proportional control, there is normally a steady-state control error. With integral action, a small positive error will always lead to an increasing control signal, and a negative error will result in a decreasing control signal, regardless of the error's size. The following simple argument shows that the steady-state error will always be zero with integral action. Assume the system is at steady state with a constant control signal (u_0) and a constant error (e_0). It follows from Equation 22 that the control signal is then given by:

$$u_0 = K\left(e_0 + \frac{e_0}{T_i}t\right) \quad [22]$$

While $e_0 \neq 0$, this clearly contradicts the hypothesis that the control signal u_0 is constant. A controller with integral action will always give zero error in steady state (Åström K. 2009).

Derivative Action

The objective of derivative action is to improve closed-loop stability. The instability mechanism can be described as follows.

Due to the dynamics of the process, it will take some time before a change in the control variable is detectable at the process output. Thus, the control system will take time to correct an error. The action of a proportional-derivative controller can be interpreted as if the control were made proportional to the predicted process output, where the prediction is made by extrapolating the error along the tangent to the error curve. The basic structure of a PD controller is:

$$u(t) = K\left(e(t) + T_d\frac{de(t)}{dt}\right) \quad [23]$$

The control signal is thus proportional to an estimate of the control error at time T_d forward, where the estimate is obtained by linear extrapolation. (Åström K. 2009. Kuo B. 1996).

Simulation of the Hall effect propulsion system in Simulink®

To simulate the different types of controllers that can be used, we employ a tool provided by Simulink® called PID Tuner. The PID Tuner app automatically adjusts the gains of a PID controller for a SISO (Single-Input Single-Output) plant to achieve a balance between performance and robustness.

This tool allows you to specify the controller type, such as PI controllers, PID controllers with a derivative filter, or PID controllers with two degrees of freedom (2-DOF). The analysis graphs allow you to examine controller performance in both the time and frequency domains. You can interactively fine-tune controller performance by adjusting loop bandwidth and phase margin, or by improving setpoint tracking or disturbance suppression.

We use PID Tuner with a plant represented by a numerical LTI model, such as a transfer function (tf) or a state-space model (ss). With Simulink® Control Design™ software, we use PID Tuner to tune a PID Controller or PID Controller (2DOF) block in a Simulink model. Using System Identification Toolbox™ software, the app can be used to estimate a plant from measured or simulated data and design a controller for the estimated plant.

ISSN: 2523-6865
RENIECYT-SECIHTI: 1702902

Aburto–Policarpo Gethsi, Castillo-Sánchez Martín and López-Cárdenas Rodrigo [2025]. Dynamic control analysis by simulation of the main components of a Hall Effect thruster. Journal Computational Simulation. 9[20] 1-17: e20920117
https://doi.org/10.35429/JCS.2025.9.20.2.1.17

This tool simulates P, I, D, PI, PD, and PID controls in that order for each transfer function related to the components of the Hall effect impeller, with the first simulated component being the magnetic field generated by a coil, followed by the voltage, and finally the injector.

Simulink components and functions used in the test simulation

For each simulation, the PID controller is first tuned. To perform this tuning and test the different controllers, various functions and tools provided by Simulink are needed, such as input and disturbance components, transfer function, and scope (visualizer), among others, which are presented below.

Unit step function

A unit step function is a mathematical function that is activated at time t = 0 and is represented by the values 1 for $t \geq 0$ and 0 for $t < 0$. It is commonly used to represent an idealized switch and can be multiplied by other functions to activate them at t = 0.

PID controller

This tool is a tuner that automatically adjusts the gains of a PID controller.

Transfer Function

In MATLAB™, a transfer function is a mathematical representation that describes the relationship between the input and output of a linear time-invariant system, especially in the context of control system analysis. It is used to model and analyze the behavior of physical systems.

$$\frac{1}{s+1} \qquad [24]$$

Scope (displayer)

A scope (oscilloscope or signal viewer) is a visual tool that allows you to observe and analyze data, especially real-time signals, during the execution of a model or program.

Sum Block

In Simulink, a Sum block is a fundamental component that performs addition or subtraction operations on its input signals. This block can handle scalar, vector, or matrix inputs and allows the addition or subtraction of these inputs.

Signal editor

The signal editor is a tool that allows you to create, edit, and manage signal scenarios for use in simulation models. It allows you to define groups of signals with different configurations and apply them to models for various simulations or tests.

PID Control Tuning

Arrangement of components for tuning

Initially, we arranged the unit step, summing point, PID controller, transfer function, and scope blocks as shown in Figure 6.

Box 6

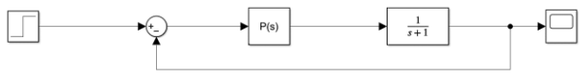

Figure 6
Control system for performing transfer function tuning

We click on our PID tuner block, which opens a window like the one shown, where we have the option to select the type of controller we want to tune. We select a P controller. Once the controller is selected, we select the "Apply" button to confirm the control, and then "Tune," which will tune the controller for the proposed transfer function (Figure 7).

Box 6

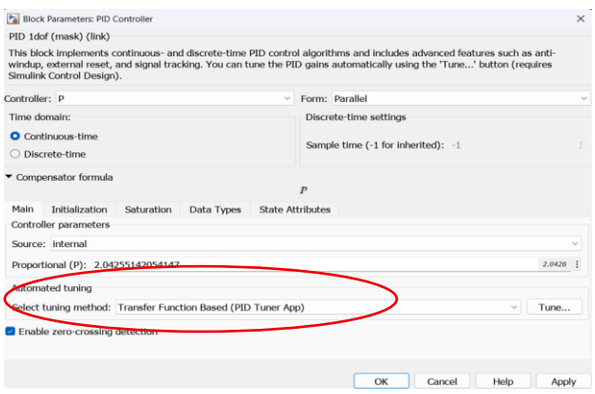

Figure 7
Controller selection, application, and tuning

ISSN: 2523-6865
RENIECYT-SECIHTI: 1702902

After selecting "Tune," a process will begin that, upon completion, will display a window where Simulink will have selected the appropriate signal response parameters. Next, select the "Update Blocks" button, which will update the P, I, and D parameters (depending on the selected control) in the controller. Once this is done, you can close this window, and you will see that the control parameters have been updated (Figures 8 and 9).

Box 8

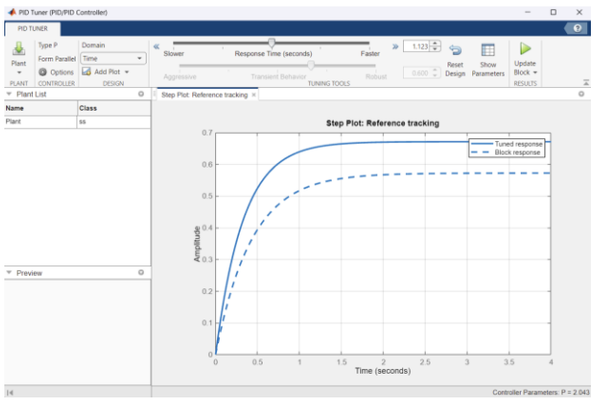

Figure 8
Tuning and application of tuning parameters

Once this process has been followed, our control block is ready to be tested with a reference signal and disturbances. (Moore H. 2007. Cubillos M. 2003).

Box 9

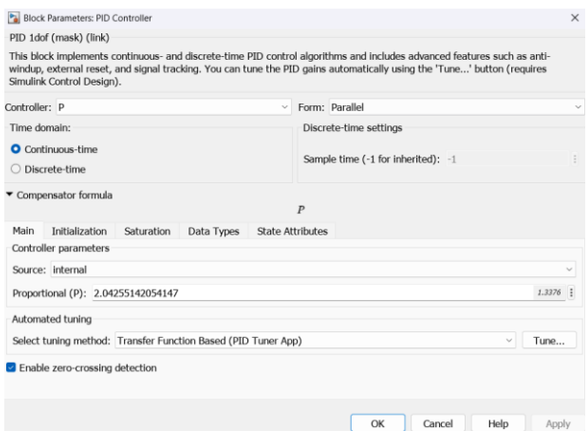

Figure 9
Definition of the Proportional, Integral and/or Derivative parameters

Results

Magnetic Field Simulation
P-Control for the Magnetic Field

Box 10

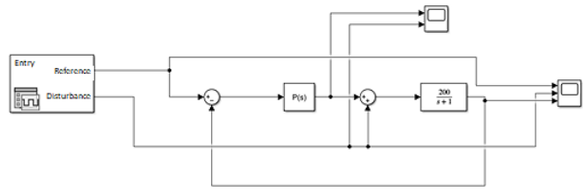

Figure 10
P control system for the magnetic field

Box 11

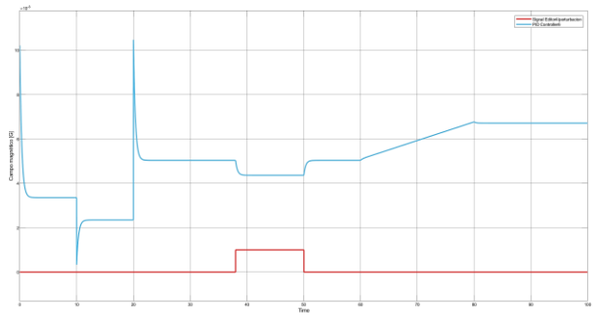

Figure 11
Graph of the perturbation response of the P controller tuned for the magnetic field

Box 12

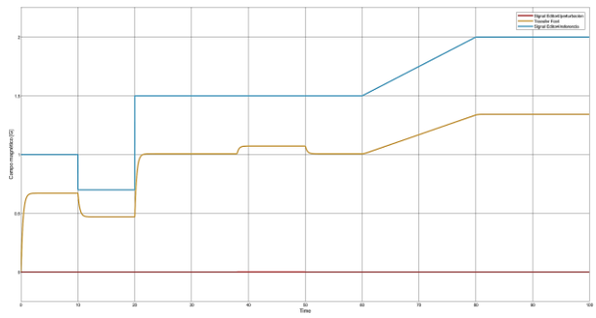

Figure 12
Graph of the magnetic field response with respect to the controller reference P

Control I for the magnetic field

Box 13

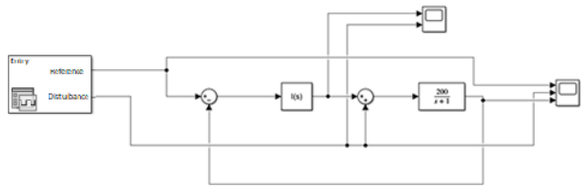

Figure 13
Control system I for the magnetic field

ISSN: 2523-6865
RENIECYT-SECIHTI: 1702902

Aburto–Policarpo Gethsi, Castillo-Sánchez Martín and López-Cárdenas Rodrigo [2025]. Dynamic control analysis by simulation of the main components of a Hall Effect thruster. Journal Computational Simulation. 9[20] 1-17: e20920117
https://doi.org/10.35429/JCS.2025.9.20.2.1.17

Box 14

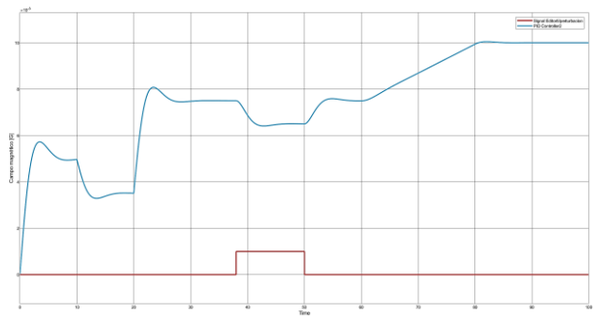

Figure 14

Graph of the disturbance response of the tuned controller I for the magnetic field

Box 15

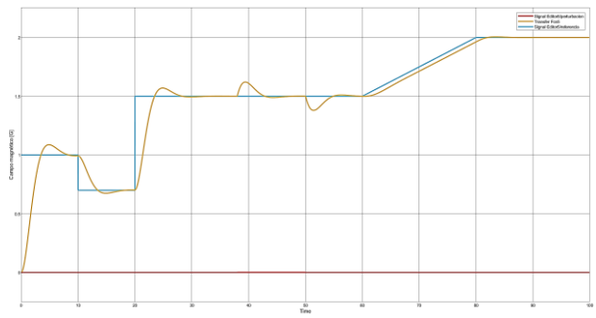

Figure 15

Graph of the magnetic field response with respect to the controller reference I.3.3.3 Control

PI for the magnetic field

Box 16

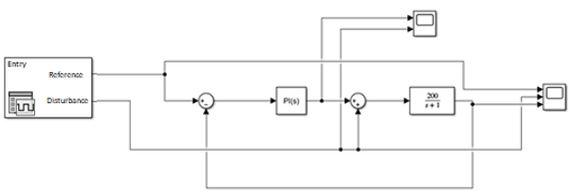

Figure 16

PI control system for the magnetic field

Box 17

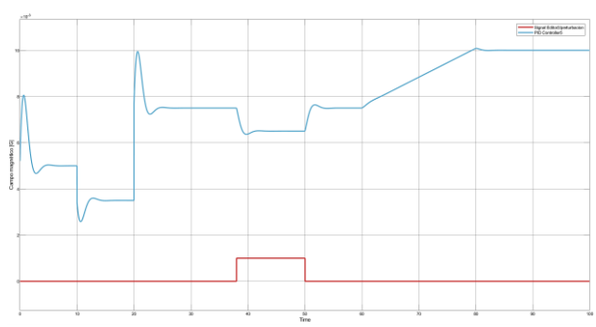

Figure 17

Graph of the disturbance response of the PI controller tuned for the magnetic field

Box 18

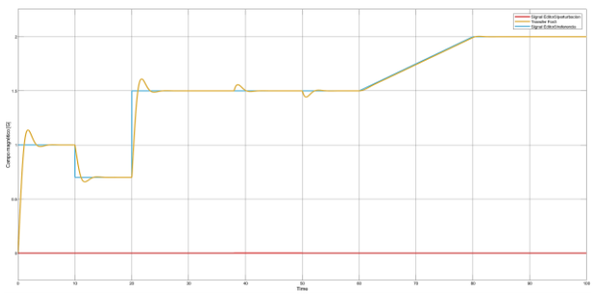

Figure 18

Graph of the magnetic field response with respect to the PI controller reference

Control for the Magnetic Field

Box 19

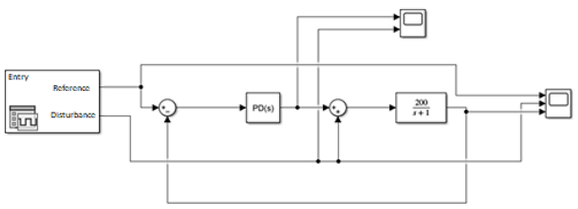

Figure 19

PD control system for the magnetic field

Box 20

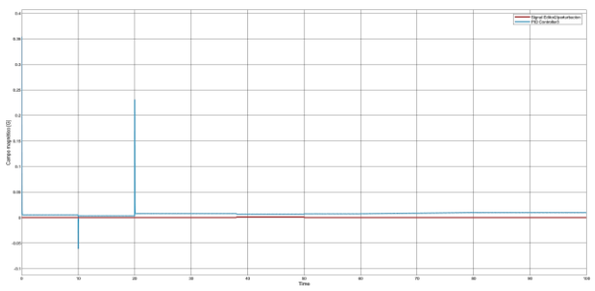

Figure 20

Graph of the disturbance response of the PD controller tuned for the magnetic field

Box 21

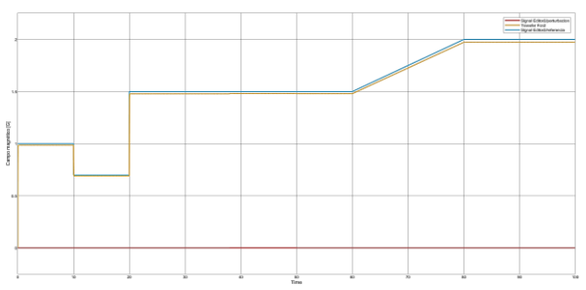

Figure 21

Graph of the magnetic field response with respect to the PD controller reference

ISSN: 2523-6865
RENIECYT-SECIHTI: 1702902

Aburto–Policarpo Gethsi, Castillo-Sánchez Martín and López-Cárdenas Rodrigo [2025]. Dynamic control analysis by simulation of the main components of a Hall Effect thruster. Journal Computational Simulation. 9[20] 1-17: e20920117
https://doi.org/10.35429/JCS.2025.9.20.2.1.17

PID control for the magnetic field

Box 22

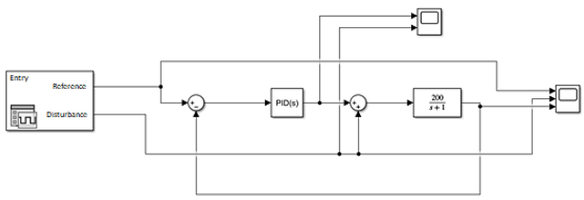

Figure 22
PID control system for the magnetic field

Box 23

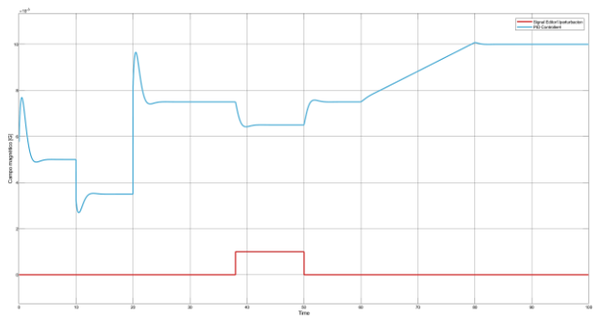

Figure 23
Graph of the disturbance response of the PID controller tuned for the magnetic field

Box 24

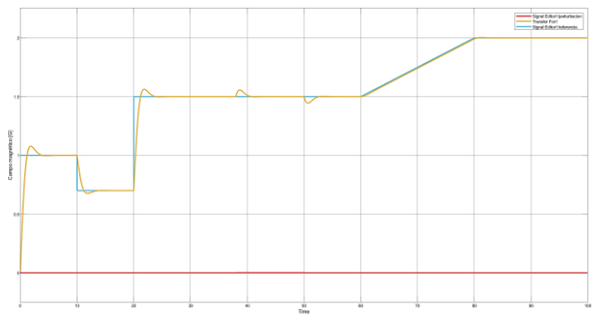

Figure 24
Graph of the magnetic field response with respect to the PID controller reference

Voltage Simulation
Voltage Control (P)

Box 25

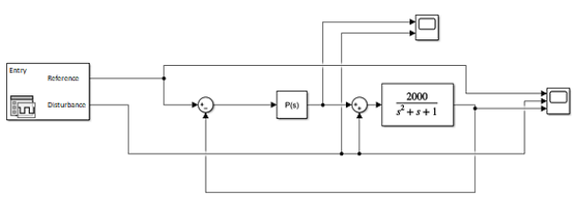

Figure 25
P control system for voltage

Box 26

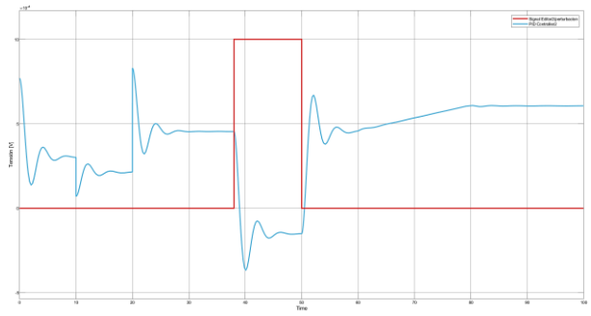

Figure 26
Graph of the disturbance response of the P controller tuned for voltage.

Box 27

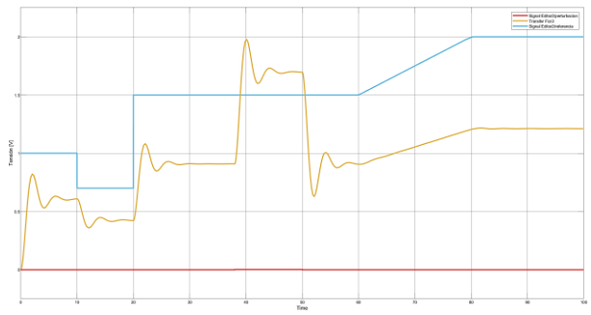

Figure 27
Graph of the voltage response with respect to the controller reference P

Voltage Control I

Box 28

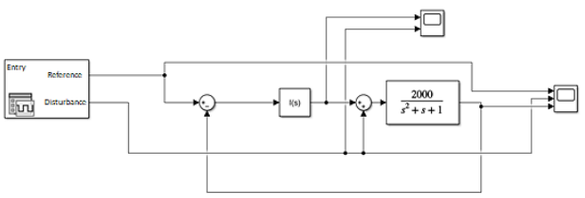

Figure 28
Control System I for voltage

Box 29

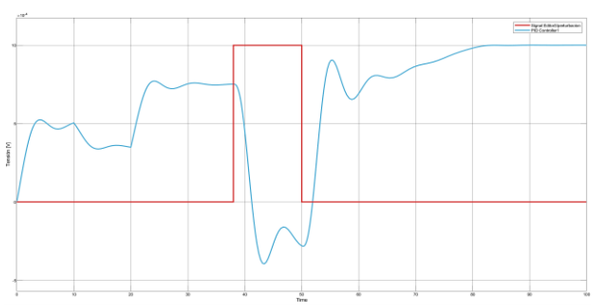

Figure 29
Graph of the disturbance response of the tuned I controller for voltage

ISSN: 2523-6865
RENIECYT-SECIHTI: 1702902

Box 30

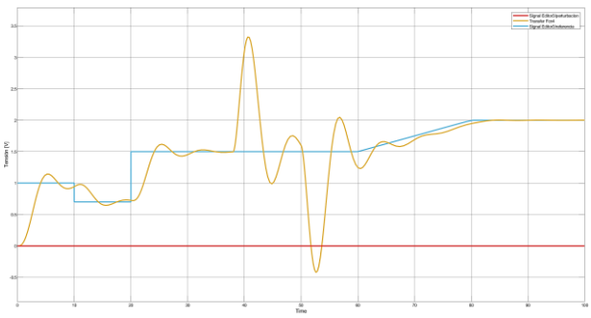

Figure 30
Graph of the voltage response with respect to the controller reference I

PI Voltage Control

Box 31

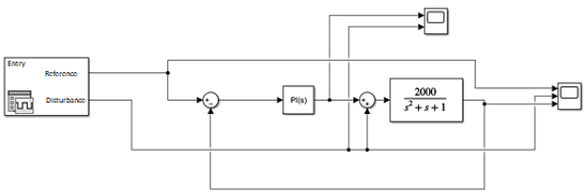

Figure 31
PI control system for voltage

Box 32

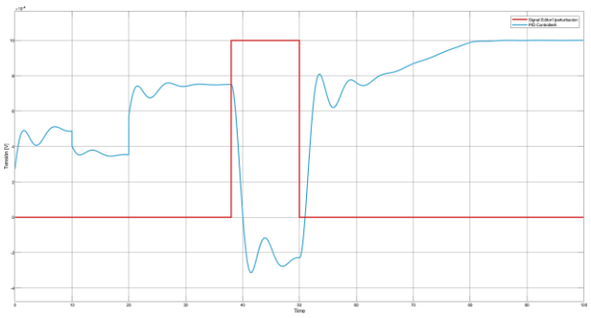

Figure 32
Graph of the disturbance response of the PI controller tuned for voltage.

Box 33

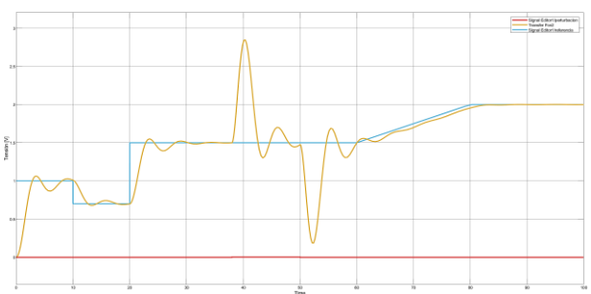

Figure 33
Graph of the voltage response with respect to the PI controller reference

PD Voltage Control

Box 34

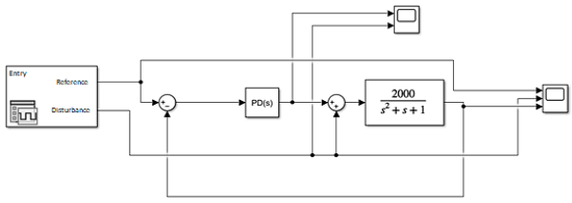

Figure 34
PD control system for voltage

Box 35

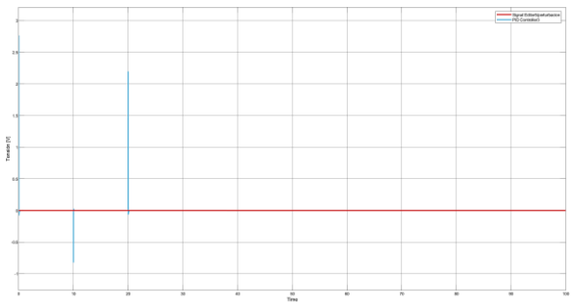

Figure 35
Graph of the disturbance response of the PD controller tuned for voltage

Box 36

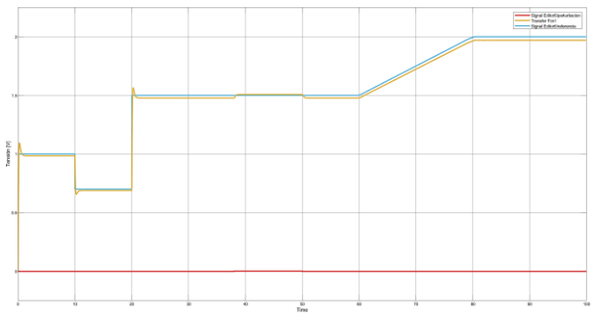

Figure 36
Graph of the voltage response with respect to the PD controller reference

PID Voltage Control

Box 37

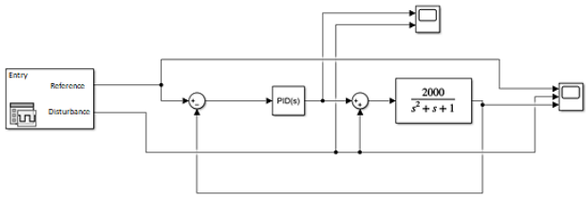

Figure 37
PID control system for voltage

ISSN: 2523-6865
RENIECYT-SECIHTI: 1702902

Aburto–Policarpo Gethsi, Castillo-Sánchez Martín and López-Cárdenas Rodrigo [2025]. Dynamic control analysis by simulation of the main components of a Hall Effect thruster. Journal Computational Simulation. 9[20] 1-17: e20920117
https://doi.org/10.35429/JCS.2025.9.20.2.1.17

Box 38

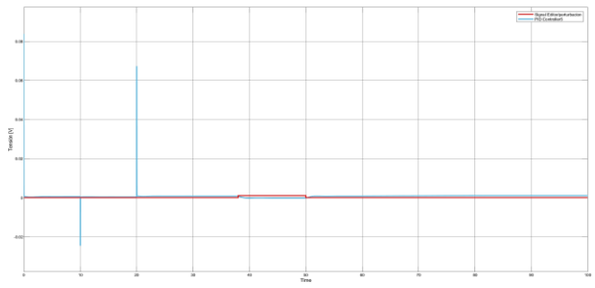

Figure 38
Graph of the disturbance response of the PID controller tuned for voltage

Box 39

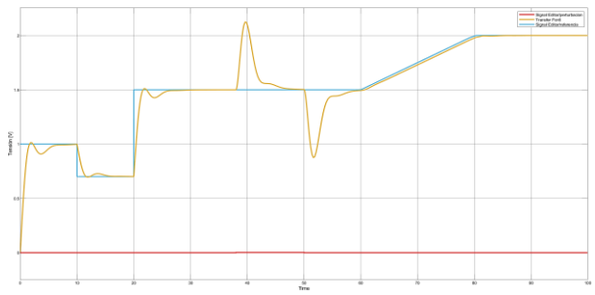

Figure 39
Graph of the voltage response with respect to the PID controller reference.

Injector Simulation

Injector P Control

Box 40

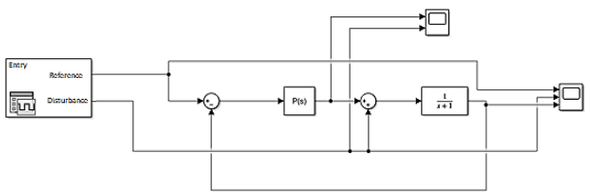

Figure 40
P control system for the injector

Box 41

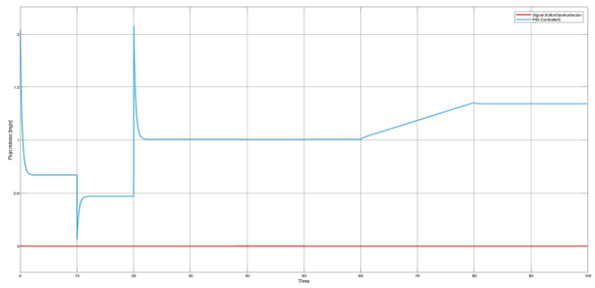

Figure 41
Graph of the disturbance response of the tuned P controller for the injector

Box 42

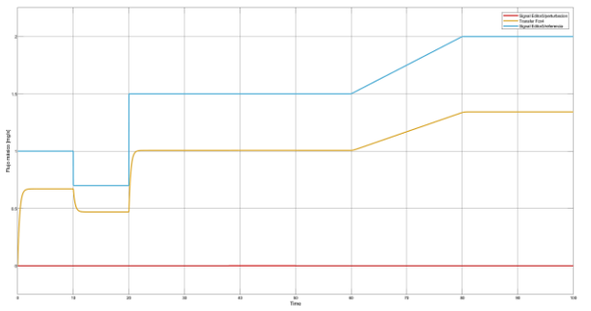

Figure 42
Graph of the injector response with respect to the controller reference P

Control I for the injector

Box 43

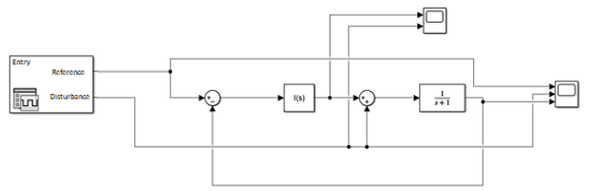

Figure 43
Control system I for the injector

Box 44

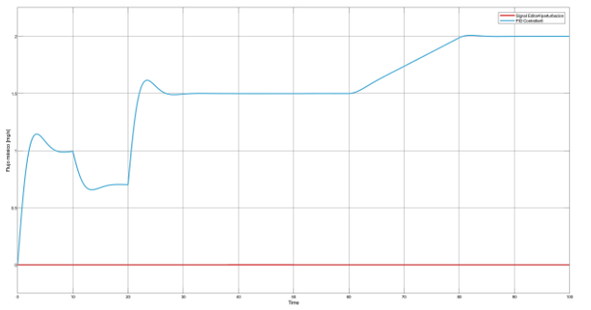

Figure 44
Graph of the disturbance response of the tuned controller I for the injector

Box 45

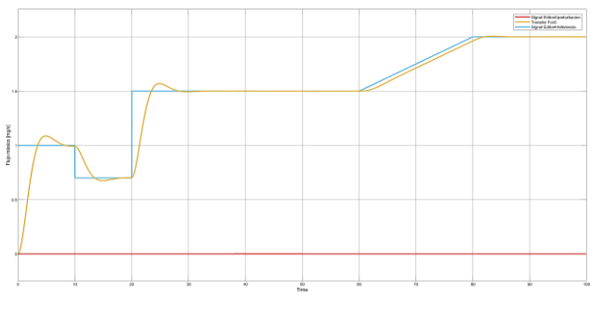

Figure 45
Graph of the injector response with respect to the controller reference I

ISSN: 2523-6865
RENIECYT-SECIHTI: 1702902

Aburto–Policarpo Gethsi, Castillo-Sánchez Martín and López-Cárdenas Rodrigo [2025]. Dynamic control analysis by simulation of the main components of a Hall Effect thruster. Journal Computational Simulation. 9[20] 1-17: e20920117
https://doi.org/10.35429/JCS.2025.9.20.2.1.17

PI Control for the Injector

Box 46

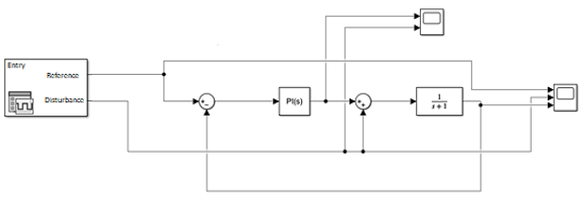

Figure 46
PI control system for the injector

Box 47

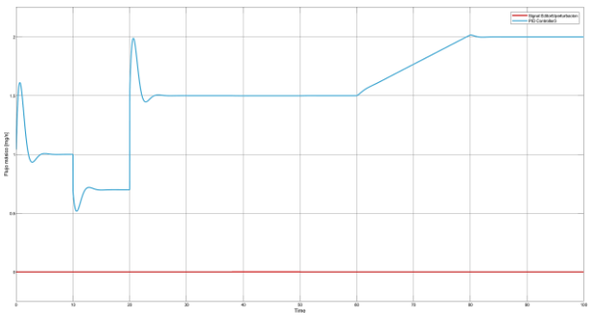

Figure 47
Graph of the disturbance response of the tuned PI controller for the injector

Box 48

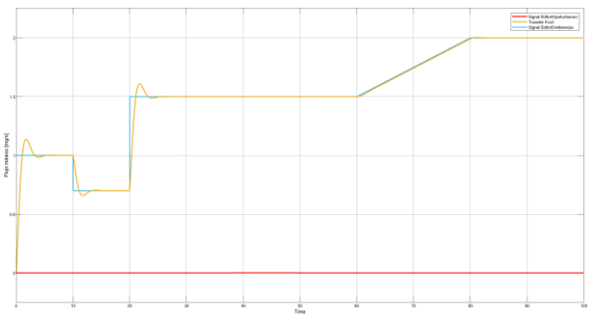

Figure 48
Graph of the injector response with respect to the PI controller reference

Control for the Injector

Box 49

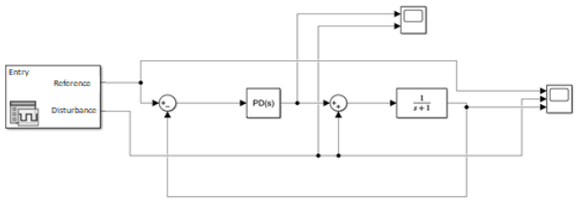

Figure 49
PD control system for the injector

Box 50

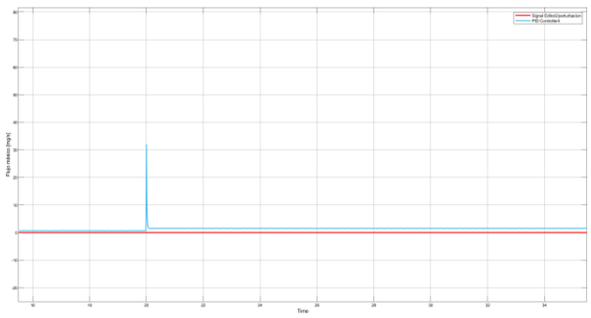

Figure 50
Graph of the disturbance response of the tuned PD controller for the injector

Box 51

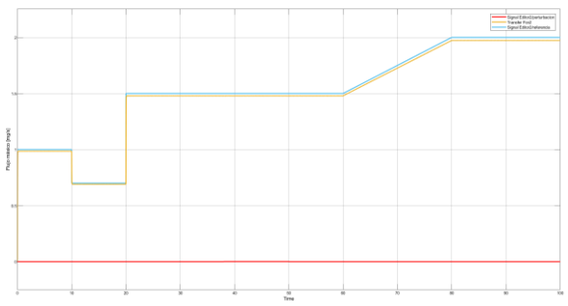

Figure 51
Graph of the injector response with respect to the PD controller reference

Control for the Injector

Box 52

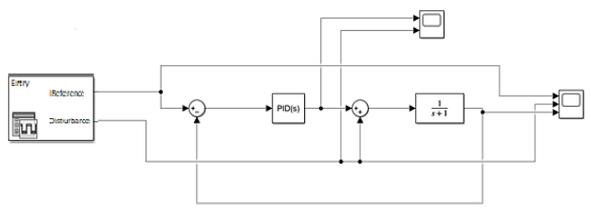

Figure 52
PID control system for the injector

Box 53

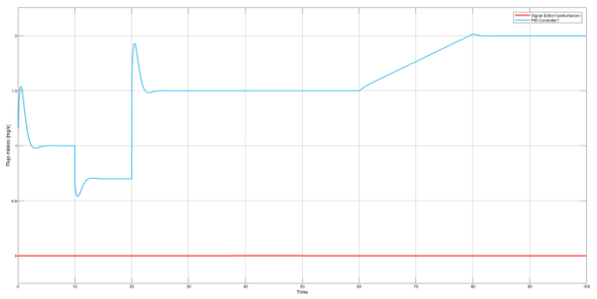

Figure 53
Graph of the disturbance response of the tuned PID controller for the injector

ISSN: 2523-6865
RENIECYT-SECIHTI: 1702902

Aburto–Policarpo Gethsi, Castillo-Sánchez Martín and López-Cárdenas Rodrigo [2025]. Dynamic control analysis by simulation of the main components of a Hall Effect thruster. Journal Computational Simulation. 9[20] 1-17: e20920117
https://doi.org/10.35429/JCS.2025.9.20.2.1.17

Box 54

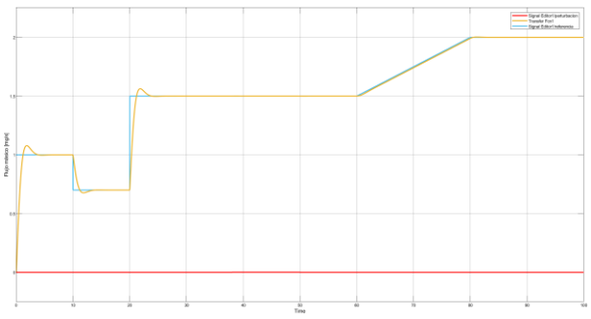

Figure 54
Graph of the injector response with respect to the PID controller reference

Results Analysis

Using the transfer equation developed by Sánchez J. (2015) in the simulation.

Based on the behavior shown in the graphs presented in the simulation for the magnetic field, we can highlight the PD, PI, and PID controllers, whose resulting behaviors most closely matched the reference signals proposed for testing the controller. However, it is also important to note that the PD controller, shown in Figure 20, exhibits a very abrupt change in its magnetic field levels within a very short time interval. Therefore, it can be deduced that this behavior is physically unachievable, and thus, attempting to implement this controller is not viable.

Regarding voltage, the simulations show efficient control in the PD and PID controllers, although they may present difficulties for physical implementation due to the sudden changes in voltage levels over a very short period of time. In contrast, the PI controller shown in Figure 32, although it exhibits irregular behavior, remains close to the reference, making physical implementation possible.

In the case of the injector, the I, D, PI, and PD controllers show behavior consistent with their respective references, making them acceptable. However, it should be noted that the PD controller cannot be implemented because it is physically impossible to make the injector re-enter the fuel. Therefore, only the I, D, and PI controllers are the most viable options for implementation.

Conclusions

Based on the simulation results, we can conclude that PI and PID controllers are best suited for regulating magnetic fields due to their precise reference tracking, unlike PD controllers, whose abrupt changes make them physically impractical. Regarding voltage control, PI controllers stand out for their balance between efficiency and physical feasibility, while PD and PID controllers, although acceptable, exhibit excessively rapid variations that hinder their practical implementation.

For the injector, the I, D, and PI controllers are the most viable, as they achieve good reference tracking without requiring physically unfeasible behaviors, such as fuel return in the case of the PD controller.

In summary, the PI controller emerges in this study as the most robust and realistic option for the three applications analyzed, combining accuracy, stability, and physical feasibility. However, in scenarios where faster tuning is prioritized, the PID controller could be considered, provided its practical limitations are evaluated.

Statements

Conflict of interest

The authors declare no conflict of interest. They have no competing financial interests or known personal relationships that could have influenced the article presented here.

Contribution per author

Aburto-Policarpo. Gethsi: Research; Writing - original draft.

Castillo-Sánchez, Martín: Conceptualization; Writing - revision and editing.

López-Cárdenas, Rodrigo: Methodology; Visualization; Data curation.

Acknowledgments

The authors thank the Instituto Politécnico Nacional and to the Escuela Superior de Ingeniería Mecánica y Eléctrica, Unidad Zacatenco the support provided for carrying out this research.

ISSN: 2523-6865
RENIECYT-SECIHTI: 1702902

Aburto–Policarpo Gethsi, Castillo-Sánchez Martín and López-Cárdenas Rodrigo [2025]. Dynamic control analysis by simulation of the main components of a Hall Effect thruster. Journal Computational Simulation. 9[20] 1-17: e20920117
https://doi.org/10.35429/JCS.2025.9.20.2.1.17

Abbreviations

DDC Direct Digital Control
DOF Degrees of Freedom
EP Electric Propulsion
HET Hall Effect Propulsion
PID Proportional-Integral-Derivative Control
SISO Single-Input Single-Output

References

Background

Goebel, D. M., & Katz, I. (2008). *Fundamentals of electric propulsion: Ion and Hall thrusters*. JPL Space and Technology Series.

Hey, F. G. (2018). Electric propulsion fundamentals. En *Micro Newton Thruster Development*. Springer Vieweg.

Moreno, L., & Castañeda, B. S. G. (2003). *Ingeniería de control: Modelado, análisis y control de sistemas* (1ª ed.). Ariel. México.

Basic

Lev, D., Kroes, R. L., Martinez-Sanchez, M., & Keidar, M. (2019). The technological and commercial expansion of electric propulsion. *Acta Astronautica, 159*, 213–227. https://doi.org/10.1016/j.actaastro.2019.03.043

ESA. (2002, julio). Electric propulsion systems programmes. Agencia Espacial Europea.

Hey, F. G. (2018). Electric propulsion fundamentals. En *Micro Newton Thruster Development*. Springer Vieweg.

Oh, B., & McAndrew, C. (2023). Design, fabrication, and testing of an undergraduate Hall effect thruster. *Journal of Electric Propulsion, 2*(6).

Poonam Tripathy (2020). Overview on electric propulsion systems. *International Journal of Scientific and Research Publications,* Volume 10, Issue 12, December 2020 422 ISSN 2250-3153.

Support

Åström, K. J., & Hägglund, T. (2009). *Control PID avanzado*. Pearson Educación.

Cubillos, M. F. (2003). *Apuntes: Introducción a Simulink. www.labcontrol.cl* DOI: 10.1002/9780470436448

García, H. M. S. (2010). *Sintonización del regulador automático de voltaje del sistema de control Basler DECS 125-15 en Micromáquinas Síncronas* [Tesis profesional, IPN, México].

Moore, H. (2007). *MATLAB para ingenieros* (1ª ed.). Pearson Educación.

Jiles, D. (2001). *Electronic properties of materials*. Nelson Thornes Ltd. https://doi.org/10.1201/9781315273365

Sánchez, J. E. M. (2015). *Diseño de un sistema de control para el propulsor Hall del microsatélite Quetzal* [Tesis de licenciatura, UNAM, México].

Differences

Sánchez, J. E. M. (2015). *Diseño de un sistema de control para el propulsor Hall del microsatélite Quetzal* [Tesis de licenciatura, UNAM, México].

ISSN: 2523-6865
RENIECYT-SECIHTI: 1702902

Aburto–Policarpo Gethsi, Castillo-Sánchez Martín and López-Cárdenas Rodrigo [2025]. Dynamic control analysis by simulation of the main components of a Hall Effect thruster. Journal Computational Simulation. 9[20] 1-17: e20920117
https://doi.org/10.35429/JCS.2025.9.20.2.1.17